Expansion of 1D Polarized Superfluids: The Fulde-Ferrell-Larkin-Ovchinnikov State Reveals Itself

Hong Lu, L. O. Baksmaty, C. J. Bolech, and Han Pu

Phys. Rev. Lett. **108**, 225302 — Published 29 May 2012

DOI: 10.1103/PhysRevLett.108.225302

Expansion of 1D polarized superfluids: The Fulde-Ferrell-Larkin-Ovchinnikov state reveals itself

Hong Lu[1], L. O. Baksmaty[1], C. J. Bolech[2,1], and Han Pu[1]
[1] *Department of Physics and Astronomy, Rice University, 6100 Main St., MS-61, Houston, TX 77005*
[2] *Department of Physics, University of Cincinnati, 345 Clifton Ct., ML-11, Cincinnati, OH 45221*
(Dated: April 23, 2012)

We study the expansion dynamics of a one dimensional polarized Fermi gas after its sudden release from confinement using both the mean-field Bogoliubov-de Gennes and the numerically unbiased Time-Evolving Block Decimation methods. Our results show that experimentally observable spin density modulations, directly related to the presence of a Fulde-Ferrell-Larkin-Ovchinnikov (FFLO) state, develop during the expansion of the cloud. Our work, therefore, provides a robust theoretical proposal for the detection of this long-sought state.

PACS numbers: 67.85.-d, 03.75.Ss, 37.10.Gh, 71.10.Fd

Since soon after the introduction of the Bardeen-Cooper-Schrieffer (BCS) theory, physicists have speculated on the fate of the superconducting pairing correlations in the presence of an externally imposed or induced polarization. This could arise from a mass imbalance of the pairing fermions such as in color superconductivity or in the vicinity of magnetic impurities within conventional superconductors. The FFLO (Fulde-Ferrell-Larkin-Ovchinnikov) [1–3] proposal posits that in such circumstances condensation of pairs with finite center-of-mass momenta will take place. Despite decades of work [4–6], this state has not been unambiguously observed. Although recent experiments [7] in one dimension (1D) confirmed important aspects of the phase diagram [8, 9], conclusive evidence of the FFLO phase was not obtained. We show here that during a non-equilibrium expansion, the polarized 1D superfluid develops strong signatures in the density profiles of the paring species which are a direct consequence of the FFLO crystalline order and constitute incontrovertible evidence.

We focus on a polarized degenerate Fermi gas confined to a 1D harmonic trap, where there is copious theoretical evidence that FFLO correlations occur and are fairly robust [10–17]. We also note that the experiments use not a single 1D trap but a loosely coupled array which allows tuning of the inter-tube coupling and thus makes it possible to study the 3D to 1D crossover physics [7]. Although a partially polarized phase was observed through direct imaging in the experiment, it is quite clear from recent work that the FFLO correlations *do not* leave a strong detectable signature on the ground state density profiles. Thus the character of the partially polarized phase remains unknown.

We consider a gas of N fermionic particles each of mass m with two spin projections labeled by $\sigma = (\uparrow, \downarrow)$ confined to a cigar-shaped harmonic trap. In accordance with the experimental situations [7, 18–22], we assume that the inter-particle interaction arises from a broad Feshbach resonance and is thus highly controllable. In these systems, the ratio of the radial ω_r and axial ω_z trapping frequencies which defines the anisotropy of the trap, $\lambda = \omega_r/\omega_z$, can be made so large that the Fermi energy E_F associated with the axial dynamics of the trap $N\hbar\omega_z$ and the temperature k_BT, are both much smaller than the energy level spacing of the radial confinement $\hbar\omega_r$ i.e., $N\hbar\omega_z, k_BT << \hbar\omega_r$ [7]. Due to the extremely rarefied nature of the gas, the atomic physics at play and the one-dimensional nature of the confinement, there are virtually no spin relaxation processes and the particles interact via s-wave scattering $g_{1\mathrm{D}}\delta(z)$. Furthermore, in addition to the total number N, the total polarization of the cloud $P = (N_\uparrow - N_\downarrow)/(N_\uparrow + N_\downarrow)$ can also be varied through independent control of the number of particles in each spin projection N_σ. Formally, this system is described by the Hamiltonian $\hat{H} = \int dz\,(H_0 + H_I)$ with:

$$\begin{aligned} H_0(z) &= \sum_\sigma \psi_\sigma^\dagger \left[-\frac{\hbar^2}{2m}\frac{\partial^2}{\partial z^2} + V_{\mathrm{trap}}(z) - \mu_\sigma \right] \psi_\sigma \\ H_I(z) &= g_{1D}\psi_\uparrow^\dagger(z)\psi_\downarrow^\dagger(z)\psi_\downarrow(z)\psi_\uparrow(z) \end{aligned} \tag{1}$$

where $\psi_\sigma(z)$ and μ_σ are fermionic field operators and the chemical potential, respectively, of atomic species with spin σ, and $V_{\mathrm{trap}}(z) = \frac{m}{2}\omega_z^2 z^2$. We define the Fermi energy, radius, momentum and temperature as $E_F = N$, $z_F = \sqrt{2E_F}$, $k_F = \sqrt{2E_F}$ and $T_F = E_F$. We measure the relative strength of the interaction with the ratio (γ) of the interaction (ϵ_I) and the kinetic (ϵ_k) energy densities. In the limit of weak interaction $\epsilon_I \sim g_{1\mathrm{D}}\rho(z)$ and $\epsilon_k \sim \rho^2(z)$ yielding:

$$\gamma = g_{1\mathrm{D}}/\rho \tag{2}$$

Our calculations are done using two methods with distinct but complementary advantages. First is the Time Evolving Block Decimation (TEBD) [23] (See Supplemental Material for details of methods), an unbiased approach that retains all important correlations. Second is the mean-field Bogoliubov-de Gennes (BdG) method, an effective-theory approach which describes the spin densities $\rho_\sigma(z)$ and the superfluid gap $\Delta(z)$ through quasiparticle wavefunctions. The BdG has the advantage that, when correct, it provides a clear picture of the

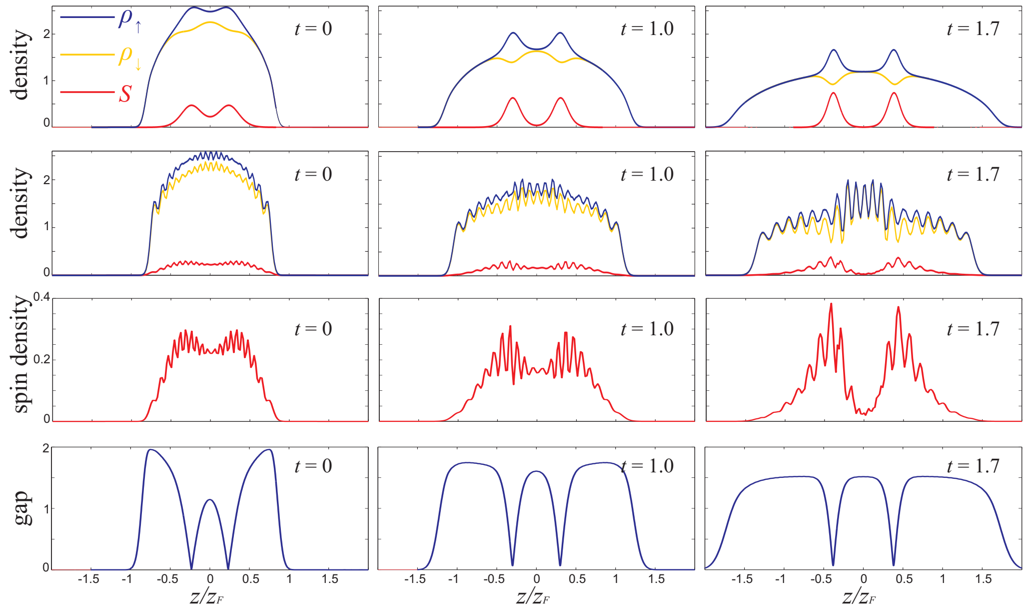

Figure 1: (color online) The expansion of a sample with $N = 40$, $P = 0.05$ and $g_{1\mathrm{D}} = -8.0$. From left to right, each column represents snapshots of the expansion dynamics at t=0.0, 1.0, 1.7 ($1/\omega_z$). Row 1 displays the density profiles. In each plot, we show $\rho_\uparrow$, $\rho_\downarrow$ and $S = \rho_\uparrow - \rho_\downarrow$ as obtained from a BdG calculation. Row 2 is the same as Row 1 except that the results are obtained from a TEBD calculation. Row 3 shows the spin densities $S(z)$ from the TEBD. Finally, in Row 4 we plot the amplitude of the superfluid gap $|\Delta|$ from the BdG calculation.

dynamics of the pairing field $\Delta(z) = g_{1\mathrm{D}}\langle\psi_\uparrow(z)\psi_\downarrow(z)\rangle$ in direct association with the particle densities $\rho_\sigma(z) = \langle\psi^\dagger_\sigma(z)\,\psi_\sigma(z)\rangle$. However, although the BdG has been observed to give a very good description of 1D samples at weak interaction [10], we do not expect this trend to extend from moderate to strong interactions. Complementarily, the TEBD method provides a stringent check for the phenomena observed in the BdG approach. In both cases we work at $T = 0$ [24] and employ a canonical approach which fixes N and P.

To observe the FFLO state, experiments must verify crystalline order in $\Delta(z)$ or, alternatively, that the average center-of-mass momentum of the pairs $\langle n_k\rangle$ is proportional to the separation of the Fermi surfaces $\langle n_k\rangle \propto k_\uparrow - k_\downarrow$. In 1D this relationship can be recast in terms of the spin density $S(z) = \rho_\uparrow(z) - \rho_\downarrow(z)$ as $\langle n_k\rangle \propto \pi \int_L S(z)dz/L$, where L is the size of the partially polarized region. Recently, a number of authors [11, 12, 25] have suggested the measurement of $\langle n_k\rangle$ — obtained from density profiles of the time-of-flight images of the expanded cloud assuming the expansion is ballistic — as the most promising avenue for detecting the finite center-of-mass momentum q of the pairs. These suggestions are extrapolations from equilibrium studies where $\langle n_k\rangle$ shows peaks at $k = \pm q$ in contrast to the peak at $k = 0$ expected for regular BCS pairing. However, we are not aware of analyses of the evolution of n_k accounting for the interacting nature of the expansion dynamics and in particular how well this signal will be preserved. This is particularly important for 1D given that γ increases during expansion [see Eq. (2)]. In this study we explore the possibility of finding a signal directly in real space. Our calculations reveal that: (1) Upon axial expansion, strong peaks develop in the spin density profiles. (2) The position of these peaks exactly coincide with the nodes in the pair correlation function and represent *prima facie* evidence of FFLO correlations. (3) The strength of this signal increases with γ and decreases with polarization, being strongest when the spin excitations are gapped. (4) The peaks in the spin density move much more slowly than the edge of the cloud.

In Fig. 1 dramatic modulation in the spin densities are observed as the cloud expands. Through a comparison of the density plots with the corresponding gap parameter $|\Delta(z)|$ (bottom row in Fig. 1) one can make a key observation: *The position and growth of the spin density peaks respectively coincide with the nodes and amplification of* $|\Delta(z)|$. Furthermore, these spin density peaks (or the order parameter nodes) move much slower during the expansion as compared to the edge of the whole cloud. We note that this is not a manifestation of the spin-charge separation as here the spin refers not to an excitation in the spin sector, but rather excess majority atoms. In fact, previous studies have indicated that, in a spin-imbalanced system, the spin and charge excitations are coupled [26].

To understand this phenomenon, it is helpful to first layout some broad features of the ground state utilizing the phase diagram for a homogeneous system together with the local density approximation (LDA) [8, 9, 14]. Under LDA, the trapped system can be regarded as locally homogeneous with a spatially varying chemical po-

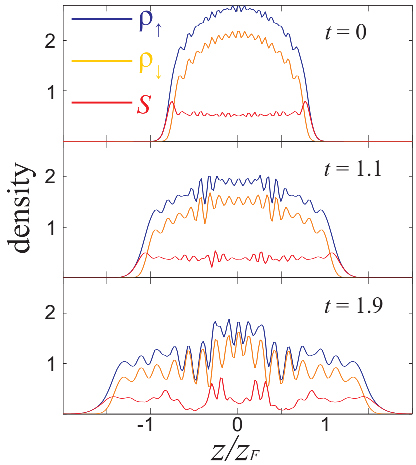

Figure 2: Density profiles, obtained from a TEBD calculation during the expansion of a sample with $N = 40$, $P = 0.15$ and $g_{1\mathrm{D}} = -8.0$.

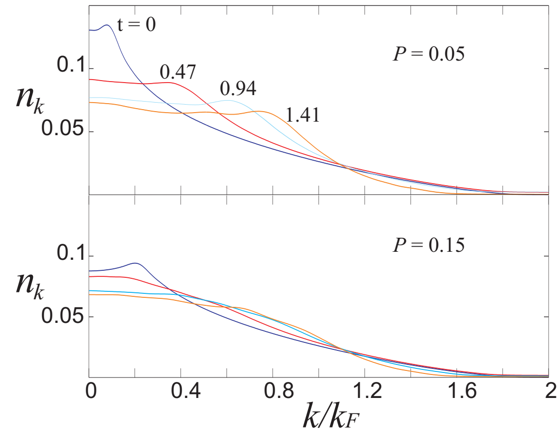

Figure 3: Pair-momentum distribution at two different polarizations for $g_{1\mathrm{D}} = -8$ and $N = 40$. In each panel, we display n_k for different times. Counting from the left, the curves correspond to $t = 0$, 0.47, 0.94 and 1.41, from top to bottom. In both cases the momentum peaks representing the FFLO state disappear from the plot during the expansion.

tential defined by: $\mu(z) = \mu_\sigma - V_{\mathrm{trap}}(z)$. There are two regimes to be considered [7, 10, 11, 13, 14] depending on whether P is smaller or larger than a critical polarization P_c. For $P < P_c$, we obtain an FFLO state at the center of the trap surrounded by fully paired BCS wings at the edges. Here the BdG calculation tells us that there is exactly one excess spin bound to each of the nodes of the order parameter and the FFLO state is analogous to a band insulator of the *relative motion* between the unpaired and paired particles. The ground state represented in Fig. 1 is within this regime and spin density peaks represent the localization of unpaired spins at the nodes of Δ. During the time of flight, the excess spins are kept pinned to the nodes of the order parameter and become more tightly bound. The dramatic effects observed occur when this localization couples with the average enhancement of $|\Delta|$ implied by an increasing γ as the density drops during expansion [see Eq. (2)]; a uniquely 1D phenomenon. Henceforth we refer to these spin peaks as node signatures.

For $P > P_c$, the FFLO state still remains at the center in the ground state, but the wings exclusively contain the majority spin component. In this regime, there are more excess spins than nodes of Δ, and consequently they are less tightly bound. Here we expect the node signatures to be less dramatic which is confirmed in Fig. 2. In particular, the spin peaks near the edges are not well resolved. We can therefore conclude that the best place to observe the node signature is at $P < P_c$, where the signal is enhanced by both a large separation of the nodes and greater contrast with the background density. We note that the value of P_c increases with $|g_{1\mathrm{D}}|$ implying a sizable observation window for the strong interactions with which experiments are conducted.

In equilibrium, the FFLO correlation appears as peaks in the pair-momentum distribution n_k defined by:

$$n_k = \frac{1}{L} \int\int dz dz' \, e^{ik(z-z')} \, O(z, z') \,, \tag{3}$$

where $O(z, z') \equiv \langle \psi_\uparrow^\dagger(z)\psi_\downarrow^\dagger(z)\psi_\downarrow(z')\psi_\uparrow(z')\rangle$ is the two-point correlation function. In Fig. 3, we observe the effects of interaction on this signature during the expansion. At sufficiently long time, n_k no longer possesses peaks at finite momentum.

One may wonder whether the node signatures can be observed in *in situ* density profiles of a trapped cloud with sufficiently large interaction strength. To answer this, we show in Fig. 4 the density profiles of a trapped system for $g_{1\mathrm{D}} = -8$, -20 and -36. (Note that for the experiment reported in Ref. [7], $g_{1\mathrm{D}} \sim -50$ for the central tube.) One can see that the modulation depth of the spin density of a trapped cloud is not very sensitive to $g_{1\mathrm{D}}$. This is in sharp contrast to the BdG calculation where the spin density modulation is indeed enhanced as γ is increased — an indication of the invalidity of the mean-field theory for strong interaction. In the exact calculation, the localization of excess spin at large $|g_{1\mathrm{D}}|$ is counter-balanced by increased quantum fluctuations neglected in the mean-field theory. Therefore, the dramatic emergence of node signatures is a unique feature of the expansion dynamics.

Finally, we address the question of the effect of the interaction strength in Fig. 5, where the spin densities in an expanding cloud are shown for two sets of interaction strength. Though the results for strong and weak interactions are qualitatively similar, the spin peaks start to develop earlier for the case of smaller $g_{1\mathrm{D}}$. This could play an important role in practice when the finite lifetime of the system must be taken into account.

In conclusion, we have investigated the expansion dy-

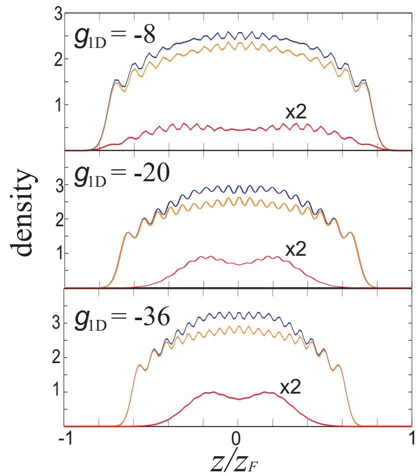

Figure 4: Ground state density profiles in trap, with $N = 40$, $P = 0.05$ and for different interaction strengths g_{1D}. In each plot, we show $\rho_\uparrow$, $\rho_\downarrow$ and S obtained from a TEBD calculation. For clarity, the spin density S is magnified by a factor of 2.

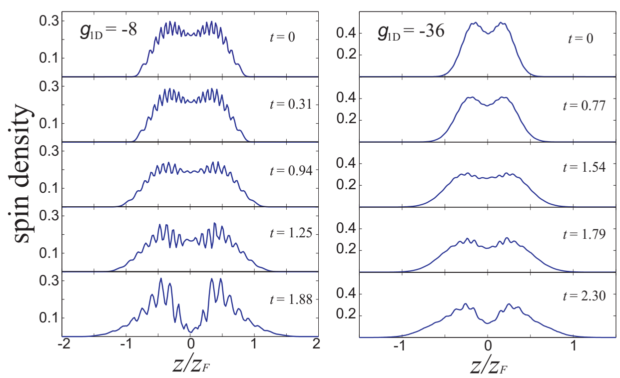

Figure 5: Expansion profiles for two different samples with $N = 40$, $P = 0.05$ but at different interaction strengths g_{1D}. In each plot, we plot the TEBD result for S. In both cases, the modulation depth of the spin density first reduces and then strengthens during the expansion.

namics of a polarized Fermi superfluid in 1D using both the BdG and TEBD methods. Our results predict that strong spin density modulations, which can be readily observed in experiment, emerge during the expansion and provide direct evidence of the FFLO state. Experimentally, an array of 1D tubes are created [7] and the measurement averages over different tubes. One obvious concern is that such an average may smear out the spin modulation. Although a full investigation of the dynamics of coupled tubes lies outside of the scope of the current work, we comment that this problem can be mitigated by allowing small inter-tube tunneling such that a quasi-1D situation results. Previous BdG studies in both a 3D cigar-shaped trap [27] and such coupled 1D tubes [28] have shown that the nodes of the order parameter (and hence the spin peaks) tend to align along the radial direction. Thus the node signature would not be smeared out by averaging. We are currently working on a 3D time-dependent BdG code which can be used to study the expansion dynamics of coupled tubes in the future. Apart from the pair-momentum distribution function described above, other methods [29] have been proposed in the literature to detect FFLO. However, they all rely on interferometric techniques requiring two fermionic superfluids, one of them being the FFLO state. Our proposal, in contrast, only requires the FFLO cloud itself and hence is significantly simpler. In a more general context, our work shows that the quantum dynamics of low-dimensional atomic gases is highly non-trivial and deserves more thorough studies in the future.

Part of the numerical calculations for this work was performed at NERSC, Navy DSRC, ARL, AFRL and the ARSC. We thank Eric Mueller, Randy Hulet, Michael Wall, Yean-an Liao and S. Bhongale for several illuminating discussions. This work is supported by the ARO Award W911NF-07-1-0464 with the funds from the DARPA OLE Program, the Welch foundation (C-1669, C-1681) and the NSF.

[1] P. Fulde, and R. A. Ferrell, Phys. Rev. **135**, A550 (1964).
[2] A. I. Larkin, and Y. N. Ovchinnikov, Zh. Eksp. Teor. Fiz. **47**, 1136 [Sov. Phys. JETP **20**, 762 (1965)].
[3] T. Mizushima, K. Machida, and M. Ichioka, Phys. Rev. Lett. **94**, 060404 (2005).
[4] A. M. Clogston, Phys. Rev. Lett. **9**, 266 (1962).
[5] B. S. Chandrasekhar, Appl. Phys. Lett. **1**, 7 (1962).
[6] R. Casalbuoni, and G. Nardulli, Rev. Mod. Phys. **76**, 263 (2004).
[7] Y.-A. Liao *et al.*, Nature (London) **467**, 567 (2010).
[8] G. Orso, Phys. Rev. Lett. **98**, 070402 (2007).
[9] P. Kakashvili, and C. J. Bolech, Phys. Rev. A **7**9, 041603 (2009).
[10] X. J. Liu, H. Hu, and P. Drummond,Phys. Rev. A **76** 043605, (2007).
[11] A. E. Feigun, and F. Heidrich-Meisner, Phys. Rev. B **76** 220508(R), (2007).
[12] M. Casula, D. M. Ceperley, and E. J. Mueller, Phys. Rev. A **7**8,033607 (2008).
[13] M. M. Parish,S. K. Baur, E. J. Mueller, and D. Huse, Phys. Rev. Lett. **99**, 250403 (2007).
[14] M. Tezuka, and M. Ueda, New J. Phys. **12**, 055029 (2010).
[15] X. W. Guan, M. T. Batchelor, C. Lee, and M. Bortz, Phys. Rev. B **76**, 085120 (2007).
[16] J. Y. Lee, and X. W. Guan, Nucl. Phys. B **853**, 125 (2011).
[17] J. Kajala, F. Massel, and P. Torma, Phys. Rev. A **84**, 041601 (2011).
[18] M. W. Zwierlein *et al.*, Science **311**, 492 (2006).
[19] G. B. Partridge *et al.*, Science **311**, 503 (2006).
[20] M. W. Zwierlein *et al.*, Nature(London) **442**, 54 (2006).
[21] S. Nascimbne *et al.*, Phys. Rev. Lett. **103**, 170402 (2009).
[22] C. A. Regal, M. A. Greiner, and D. S. Jin, Phys. Rev. Lett. **92**, 040403 (2004).
[23] G. Vidal, Phys. Rev. Lett. **93**, 040502 (2004).
[24] Finite temperature cannot be readily dealt with in TEBD. However, we performed finite-temperature cal-

culations using BdG and found no qualitative difference as long as the system remains in a superfluid phase.
[25] K. Yang, Phys. Rev. Lett. **95**, 218903 (2005).
[26] C. Kollath, and U. Schollwöck, New J. Phys. **8**, 220 (2006); E. Zhao, and V.W. Liu, Phys. Rev. A **78**, 063605 (2008); M. Rizzi *et al.*, Phys. Rev. B **77**, 245105 (2008).
[27] L.O. Baksmaty *et al.*, Phys. Rev. A **83**, 023604 (2011); New J. Phys. **13**, 055014 (2011).
[28] K. Sun, and C.J. Bolech, arXiv:1112.1622.
[29] V. Gritsev, E. Demler, and A. Polkovnikov, Phys. Rev. A **78**, 063624 (2008); H. Hu, and X.-J. Liu, Phys. Rev. A **83**, 013631 (2011); M. Swanson, Y. L. Loh, and N. Trivedi, arXiv:1106.3908.